PHYSICAL REVIEW C VOLUME 49, NUMBER 5 MAY 1994

Coulomb reacceleration as a clock for nuclear reactions: A two-dimensional model

C. A. Bertulani
Gesellschaft für Schwerionenforschung, KPII, Planckstrasse 1, D-64291 Darmstadt, Germany
G. F. Bertsch
Department of Physics and Institute for Nuclear Theory FM-15, University of Washington, Seattle, Washington 98195
(Received 24 January 1994)

Reacceleration effects in the Coulomb breakup of nuclei are modeled with the two-dimensional time-dependent Schrödinger equation, extending a previous one-dimensional study. The present model better describes the individual contributions of longitudinal and transverse forces to the breakup and reacceleration. Reacceleration effects are found to preserve a strong memory of the pre-breakup phase of the reaction, as was concluded with the one-dimensional model.

PACS number(s): 25.70.De, 25.70.Ef, 25.70.Mn, 24.10.−i

When a nucleus is Coulomb excited to a resonance and then decays by fragmentation, the fragments are accelerated by the Coulomb field, and final velocity distribution depends on the decay time of the resonance. In a previous work [1], this dependence was studied to see whether the reacceleration could be used as a clock for the resonance lifetime. The study was motivated by a recent experiment [2] in which the Coulomb breakup of the loosely bound nucleus ^{11}Li was measured. In that experiment it was found that the ^{9}Li fragments have on average a higher velocity than the beam velocity. This has been interpreted as a direct transition from the ground state of the projectile to free fragments in the continuum, followed by the Coulomb reacceleration of the fragments. Based on this argument the existence of a continuum resonance in ^{11}Li was questioned. A resonance would live long enough to decay far out from the target where Coulomb reacceleration effects would be negligible [2]. Besides the above-mentioned experiment, the Coulomb reacceleration effect is important in many other situations. The Coulomb breakup of ^{8}B into p+^{7}Be fragments can give information about the radiative capture reaction ^{7}Be$(p,\ \gamma)^{8}$B useful to the solar neutrino problem [3]. In the Coulomb breakup process ^{8}B is excited to a state in the continuum, decaying by a proton tunneling through the Coulomb barrier. In this case it is important to know if the time delay for the tunneling allows the Coulomb reacceleration to be neglected.

As has been shown in our previous work a clear separation between the two stages of the reaction, the excitation to the continuum and the reacceleration of the fragments, is not always possible in quantum mechanics. To show this in a simple model we have solved the Schrödinger equation nonperturbatively for a particle initially bound in a potential well. Two different potentials were used: one potential accommodated a single bound state and with no continuum resonance, and another had a single bound state but with a low-energy resonance as well.

In this Brief Report we extend the model of Ref. [1] by including part of the dynamical potential which was neglected, namely, the longitudinal Coulomb potential. To be more precise, as in Ref. [1], we solve the time-dependent Schrödinger equation

$$-\frac{\hbar^2}{2m_0}\nabla^2\Psi + V_N(r)\Psi + V_{\rm ex}(\mathbf{r},\ t)\Psi = i\hbar\ \frac{d\Psi}{dt} \qquad (1)$$

for a proton in a spherically symmetric nuclear well, $V_N(r)$. We treat the dynamics in the frame of the projectile, so that the potential well $V_N(r)$ is fixed in space. For collisions at high energies the projectile moves almost along a straight line in the target Coulomb field. We may then separate the Coulomb field into its transverse and longitudinal components. The time-dependent interaction potential of a unit charge with these fields is given by

$$V_{\rm ex}(\mathbf{r},t) = \frac{Z_T e^2}{(b^2+v^2t^2)^{3/2}}\ \mathbf{r}\ \cdot\ \mathbf{R}, \qquad (2)$$

where b is the impact parameter, v is the projectile velocity, and $\mathbf{R} \equiv (\mathbf{b},\ vt)$ is the position of the Coulomb scatterer.

We now expand the proton wave function in polar coordinates $(\mathbf{r},\ \theta)$:

$$\Psi(\mathbf{r},\ t) = \frac{1}{\sqrt{2\pi r}}\sum_m u_m(r,\ t)\ e^{im\theta}\ . \qquad (3)$$

Inserting this expansion in the Schrödinger equation one gets

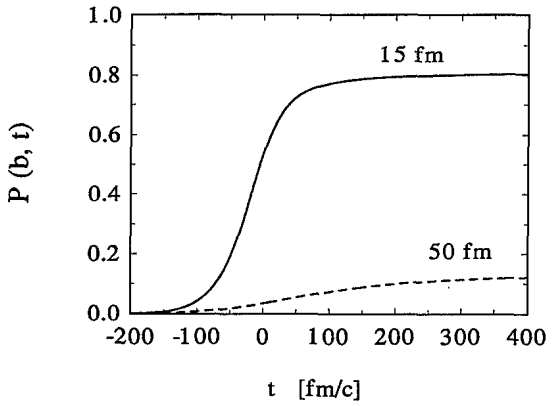

FIG. 1. Transition probability for a bound particle in a square-well to a continuum state due to a perturbing Coulomb potential, as a function of the collision time. The solid (dashed) curve corresponds to impact parameter $b = 15$ (50) fm.

$$i\hbar\frac{\partial u_m(r,t)}{\partial t} = -\frac{\hbar^2}{2m_0}\frac{\partial^2 u_m}{\partial r^2}(r,t) + V_m(r)\,u_m(r,t) + V^{(-)}(r,t)\,u_{m-1}(r,t) + V^{(+)}(r,t)\,u_{m+1}(r,t)\ , \tag{4}$$

where

$$V_m(r) = V_N(r) + \frac{\hbar^2(m^2-1/4)}{2m_0r^2},$$
$$V^{(\pm)}(r,t) = \frac{r}{2}\left[E_\parallel(t) \pm i\,E_\perp(t)\right],$$
$$E_\perp(t) = \frac{Z_T e^2\,b}{\left(b^2+v^2t^2\right)^{3/2}},$$
$$E_\parallel(t) = E_\perp(t)\,\frac{vt}{b}\ . \tag{5}$$

We solve Eq. (4) by a finite difference method, calculating the wave function at time $t+\Delta t$ in terms of the wave function at time t, according to the algorithm

$$u_m(t+\Delta t) = \left[\frac{1}{i\tau} - \Delta^{(2)} + \frac{\Delta t}{2\hbar\tau}\,V_m\right]^{-1}\left[\frac{1}{i\tau} + \Delta^{(2)} - \frac{\Delta t}{2\hbar\tau}\,V_m + \frac{\Delta t}{\hbar\tau}\,S_m(t)\right]u_m(t)\ . \tag{6}$$

In this equation $\tau = \hbar\Delta t/4m_0(\Delta x)^2$ and $S_m(t) = V^{(-)}\,u_{m-1} + V^{(+)}\,u_{m+1}$. The second difference operator $\Delta^{(2)}$ is defined as

$$\Delta^{(2)}u_m^{(j)} = u_m^{(j+1)}(t) + u_m^{(j-1)}(t) - 2u_m^{(j)}(t)\ , \tag{7}$$

with $u_m^{(j)} \equiv u_m(r_j,\ t)$.

The essential difference between the problem of solving the above equation and the one studied in Ref. [1] is the presence of the term $S_m(t)$ which couples u_m with u_{m+1} and u_{m-1}. This particular form of coupling is a consequence of the dipole approximation. The method of solution is the same as in Ref. [1], except that we have now a set of coupled equations for each $u_m^{(j)}(t)$.

We next define a potential V_N to have a weakly bound ground state. It is convenient to choose a square-well potential. We take depth and radius parameters to be −3.95 MeV and 3.2 fm, respectively, which produces a a single bound state of energy $E = -0.3$ MeV and root-mean-square extension of 6 fm. For the Coulomb excitation, we assume a projectile velocity of $v = c/4$, corresponding to a laboratory energy $E_{\rm lab} \sim 30$ MeV/nucleon, and a target charge corresponding to Pb, $Z_T = 82$. A grid adequate for our purposes has 500 spatial mesh points separated by 0.2 fm and 1000 time mesh points separated by 1 fm/c. The angular expansion is limited to values of m in the range $-8, -7, ..., 7, 8$.

In Fig. 1 we show the transition probability calculated from the wave function overlap

$$P(b,\ t) = 1 - \left|\langle\Psi(t)|\Psi_0\rangle\right|^2\ . \tag{8}$$

Here Ψ_0 is the ground-state wave function, and also is taken to be the initial wave function at the start of the numerical integration $t = -200$ fm/c. As time evolves the wave function acquires components in the continuum and the transition probability increases with time. Figure 1 shows the results for a collision with an impact parameter $b = 15$ fm (solid line) and $b = 50$ fm (dashed line). The transition occurs over a time interval $\Delta t \sim b/v$. The result for $b = 50$ fm is close to the perturbative Coulomb excitation calculation, but the probability at $b = 15$ fm approaches unity and a perturbative calculation is inaccurate.

In Fig. 2 we plot the particle probability density as a function of the radial position at several instants of time. The impact parameter here is $b = 15$ fm. The solid line corresponds to the ground state, normalized to unity. The dashed lines represent the free particle densities and were obtained by removing the ground-state part from the time-dependent wave function, i.e.,

$$\Psi_c = \mathcal{N}\left[\Psi(t) - \langle\Psi(t)|\Psi_0\rangle\ \Psi_0\right], \tag{9}$$

where $\mathcal{N}$ normalizes the continuum wave function, Ψ_c, to unity. It may be seen from the figure that as time evolves the particle leaves the domain of the nuclear potential. There is also a small probability that a part of the continuum wave function stays initially inside the well, due

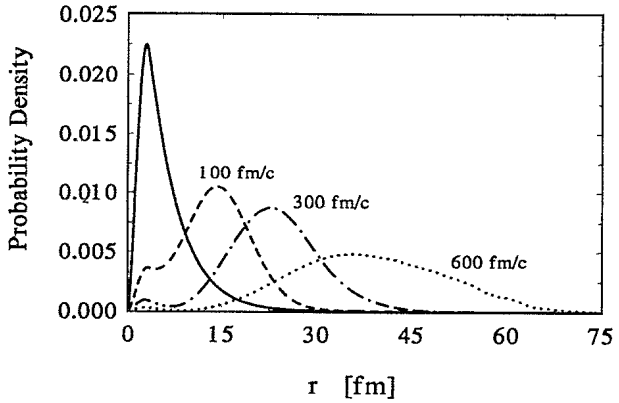

FIG. 2. Particle density distribution for the ground state (solid line) and continuum states at several instants and as a function of the radial position. The impact parameter in this collision is $b = 15$ fm.

to the reflection on the edge of the square-well potential. As the particle moves, it gets more dispersed in position, as expected. At $t = 600$ fm/c the transition probability reaches its asymptotic value and the wave packet is far from the well.

The above features are similar to what we have found previously with our one-dimensional model [1]. Special features of the higher dimension that we consider here show up in the calculation of the momentum shift associated with the net momentum that the particle gains by the reacceleration in the Coulomb field of the target. In terms of the radial wave functions u_m, at a time t, the longitudinal and the transverse components of its momentum are, respectively,

$$p_{\parallel} = -\frac{\hbar}{2} \sum_m \int dr \left[u_{m+1}(r) - u_{m-1}(r)\right]^* \frac{du_m}{dr}(r) + \frac{\hbar}{2} \sum_m m \int dr \left[u_{m+1}(r) + u_{m+1}(r)\right]^* \frac{1}{r} u_m(r) \tag{10}$$

and

$$p_{\perp} = -i \frac{\hbar}{2} \sum_m \int dr \left[u_{m+1}(r) + u_{m-1}(r)\right]^* \frac{du_m}{dr}(r) + i \frac{\hbar}{2} \sum_m m \int dr \left[u_{m+1}(r) - u_{m+1}(r)\right]^* \frac{1}{r} u_m(r) , \tag{11}$$

In Fig. 3 we show the transverse and longitudinal momenta shifts calculated by using the above formulas on the spatial grid, as a function of the impact parameter b. The solid line is the classical momentum which would be transferred to a free particle,

$$p_{\text{class}} = \int_{-\infty}^{\infty} E_{\perp}(t)dt = 2Z_T e^2/bv$$

in the transverse direction. The transverse momentum (dashed line) obtained with our nonperturbative approach follows the trend of the classical momentum. If the particle would be free after passing the distance of closest approach this quantity should be half of p_{class}. But for small impact parameters, the quantum calculation gives a momentum transfer is closer to the full p_{class}, showing that the acceleration takes place over the full trajectory, not just during the post-breakup phase.

Classically, the expected longitudinal momentum transfer is also $p_{\text{class}}/2$ for a particle emitted at $t = 0$. The quantum results are smaller than this, because the deceleration force for $t < 0$ is remembered in the quantum amplitude. Thus, a purely classical model for the breakup is not able to explain the correct magnitude of the momentum shifts since an exact definition of the position of the breakup is not possible quantum mechanically.

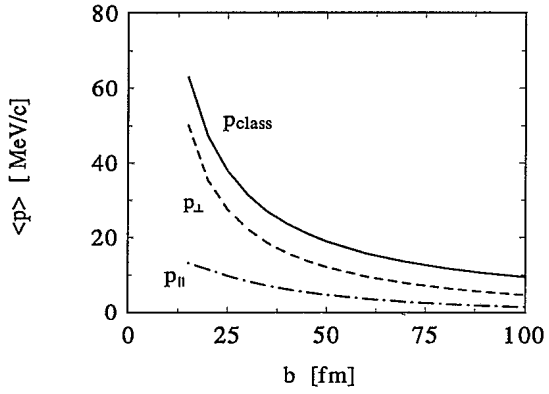

FIG. 3. Momentum shift of the continuum particle excited from the square-well potential as a function of the impact parameter. The solid, dashed, and dash-dotted curve are the classical, transverse, and longitudinal momentum, respectively.

In Fig. 4 we show the occupation probabilities of the different m states for a collision with (a) $b = 15$ fm and (b) $b = 50$ fm. The probability is normalized to one particle in the continuum. For collisions at small impact parameters the excitation probability is large and the particle initially jumps into the $m = \pm 1$ states due to the coupling S_m in Eq. (6), but as the excitation probability increases other neighboring m values are sequentially excited. Due to the angular momentum transfer in the collision, positive m values are favored, resulting in a net angular momentum for the free particle. For large impact parameters the small excitation probability makes that essentially the states with $m = \pm 1$ are populated, in agreement with the result of first-order perturbation theory. At $b = 50$ fm the reacceleration effect is still appreciable and the state with $m = 1$ is more populated than the $m = -1$. The reacceleration effect causes a depopulation of the $m = -1$ state which occurs via the

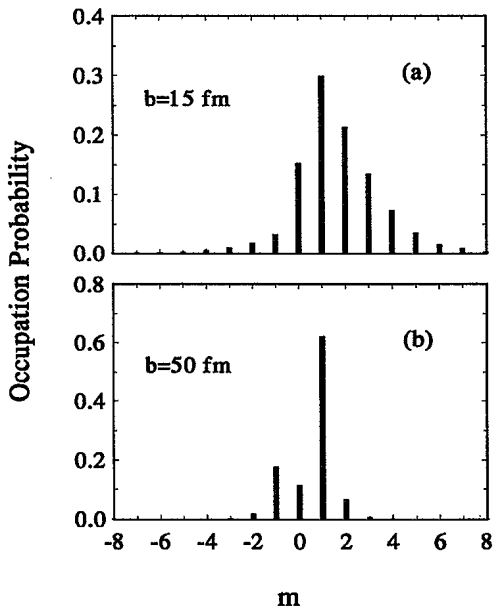

FIG. 4. Occupation probability for several angular momentum states, m, in the continuum of a square-well potential. (a) [(b)] is for b=15 [50] fm.

$m = 0$ state to the $m = 1$ state.

We now consider the case where the Hamiltonian contains a resonance as well as a bound state. We use a square well shape with rectangular barrier to produce the resonance. The parameters that we use are $V_0 = 9$ MeV for the depth of the well, a_0=4 fm for the range of the well, $V_1 = 5$ MeV for the height of the barrier, and $a_1 = 3$ fm for the width of the barrier. This potential has a bound state at $E = -3.7$ MeV and a resonant state, with $m = 1$, at 1 MeV and a width of 0.5 MeV. These properties may be deduced from the decomposition of the time-dependent wave function into energy eigenstates (see discussion in [1]). The 0.5 MeV width of the resonance translates into a mean lifetime of 400 fm/c, allowing to the projectile to travel 80 fm beyond the point of excitation. For impact parameters of the order of 15 fm, the classical reacceleration following breakup will be very small and we expect the momentum of the emitted particle to be nearly zero.

The results of the quantum treatment are shown in Fig. 5 for the transverse (dashed curve) and longitudinal (dashed-dotted curve) momentum. The classical momentum is shown by the solid line. Very different features are observed as compared to our previous one dimensional model. First, the transverse momentum is smaller than what one obtains in the one-dimensional model (Fig. 7 of [1]). Obviously, coherence effects in the wave function are very important for this observable. Second, we observe that the momentum shifts do not decrease steadily, but have a small bump at $b \sim 50$ fm. This can be understood as a resonant effect. The time-dependent Coulomb fields given by Eq. (2) contain Fourier components peaked around $\omega \sim v/b$. At $b = 50$ fm this corresponds to an energy approximately equal to 1 MeV, i.e., the energy of the resonant state. Thus, for $b \sim 50$ fm the action of the force is resonant with the excitation energy. This feature would also be seen in Fig. 7 of Ref. [1], if it would be extended to larger values of b. This has been checked numerically. Another interesting result is that for b greater than 40 fm the reacceleration caused by the longitudinal field is larger than that caused by the transverse field. The longitudinal reacceleration is significant over the entire range of impact parameters, despite the long lifetime of the resonance. This accords qualitatively with the experimental finding [2] that the reacceleration effect is present despite an expected lifetime of the order of that in our model.

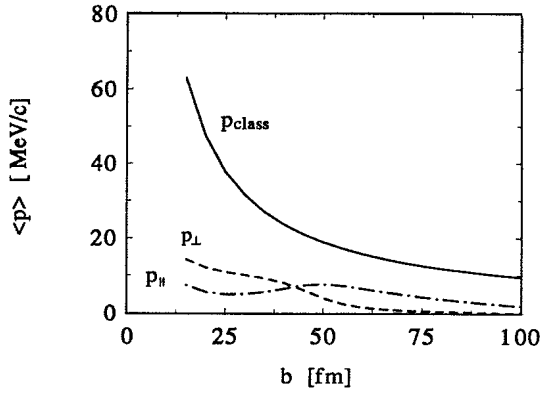

FIG. 5. Momentum shift of the continuum particle excited from the square-barrier potential as a function of the impact parameter. The solid, dashed, and dash-dotted curve are the classical, transverse, and longitudinal momentum, respectively.

In conclusion, we have studied the effect of the reacceleration of a particle following a breakup in the nuclear Coulomb field. We find that the effect is intrinsically quantum mechanical and the disentangling of prior- and post-breakup phase of the reaction is not well defined. We have seen that the longitudinal Coulomb field is very important for the reacceleration effect and cannot be neglected in the calculations. Qualitatively we find some suppression of the reacceleration when the particle is excited to a narrow resonance. This clearly shows that the time delay in emitting the particle can play an important role, although one that does not seem to be easy to estimate. Another possible signature of a resonant state could be obtained by looking into the impact parameter dependence of the momentum shift. As we have seen, when the inverse of the collision time is approximately equal to the energy of the state an appreciable deviation of the momentum shift from a monotonously decreasing dependence on the impact parameter should be observed.

This work was supported in part by the Department of Energy under Grant No. DE-FG06-90ER40561.

[1] G.F. Bertsch and C.A. Bertulani, Nucl. Phys. **A556**, 136 (1993).

[2] K. Ieki *et al.*, Phys. Rev. Lett. **70**, 730 (1993); D. Sackett *et al.*, Phys. Rev. C **48**, 118 (1993).

[3] T. Motobayashi *et al.*, Rikkyo Report No. RUP 94-2, 1994 (unpublished); M. Gai (private communication).